DTU Library

Advanced Control Strategy of DFIG Wind Turbines for Power System Fault Ride Through

Yang, Lihui; Xu, Zhao; Ostergaard, Jacob; Dong, Zhao Yang; Wong, Kit Po

Link back to DTU Orbit

Advanced Control Strategy of DFIG Wind Turbines for Power System Fault Ride Through

Lihui Yang, Zhao Xu, *Member, IEEE*, Jacob Østergaard, *Senior Member, IEEE*,
Zhao Yang Dong, *Senior Member, IEEE*, and Kit Po Wong, *Fellow, IEEE*

Abstract—**This paper presents an advanced control strategy for the rotor and grid side converters of the doubly fed induction generator (DFIG) based wind turbine (WT) to enhance the low-voltage ride-through (LVRT) capability according to the grid connection requirement. Within the new control strategy, the rotor side controller can convert the imbalanced power into the kinetic energy of the WT by increasing its rotor speed, when a low voltage due to a grid fault occurs at, e.g., the point of common coupling (PCC). The proposed grid side control scheme introduces a compensation term reflecting the instantaneous DC-link current of the rotor side converter in order to smooth the DC-link voltage fluctuations during the grid fault. A major difference from other methods is that the proposed control strategy can absorb the additional kinetic energy during the fault conditions, and significantly reduce the oscillations in the stator and rotor currents and the DC bus voltage. The effectiveness of the proposed control strategy has been demonstrated through various simulation cases. Compared with conventional crowbar protection, the proposed control method can not only improve the LVRT capability of the DFIG WT, but also help maintaining continuous active and reactive power control of the DFIG during the grid faults.**

Index Terms—**Doubly fed induction generator (DFIG), low voltage ride through, power system fault, wind turbine.**

I. INTRODUCTION

DOUBLY fed induction generator (DFIG) is a popular wind turbine (WT) system due to its high energy efficiency, reduced mechanical stress on the WT, and relatively low power rating of the connected power electronics converter of low costs. With increasing penetration level of WTs into the grid, the wind

power grid connection codes in most countries require that WTs should remain connected to the grid to maintain the reliability during and after a short-term fault [1]. The ability of WT to stay connected to the grid during voltage dips is termed as the low-voltage ride-through (LVRT) capability.

In order to fulfill the LVRT requirement for DFIG WTs, there are two major issues to be addressed properly under a fault condition. The first one is the over-current that can occur in rotor and stator circuits, while the second one is the DC-link over-voltage. Both can be attributed to the excessive energy that cannot be transmitted into the grid during the faults. As the power electronics converters in the DFIG system have relative lower power rating compared with the WT with fully rated converters, the LVRT capability of the DFIG WT is of special interest with respect to the stability issue of such system. Quite a few studies have been carried out to improve the LVRT capability of the DFIG WT [3]–[19].

Among the available control strategies, the crowbar protection is the mostly used. During the faults, the rotor side converter will be blocked, and the crowbar circuit, installed across the rotor terminals, will be triggered to damp the over-current in the rotor circuit. Consequently, the generator operates as a conventional induction machine, which absorbs reactive power from the faulted grid [2]. The chopper circuit, with a resistor across the DC bus, is usually used along with the crowbar to smooth the DC-link voltage by dissipating the excessive power over the DC bus [3], [4].

Based on the conventional crowbar protection, some improved crowbar solutions have been proposed to enhance the LVRT performance of the DFIG WT [5]–[10]. Although the crowbar circuits are able to protect the machine and the converter during the faults, the controllability of the rotor converter with respect to the active and reactive power of the DFIG is temporarily lost. Moreover, the usage of crowbar and chopper actually installs extra hardware in the DFIG that can increase the costs and decrease the system reliability.

Considering these drawbacks, some researchers have proposed new solutions for reducing the inrush currents in the rotor as well as the DC-link over-voltage during the faults, by means of designing more advanced control strategies for the rotor and grid side converters [11]–[19]. However, some of these algorithms are too complicated to implement in industrial applications and depend strongly on the proper design of the control parameters or the estimation of certain parameters, which may have adverse effects on its robustness.

This paper presents an innovative control strategy for both the rotor and grid side converters to enhance the LVRT capacity of the DFIG WT, without the need of additional current and
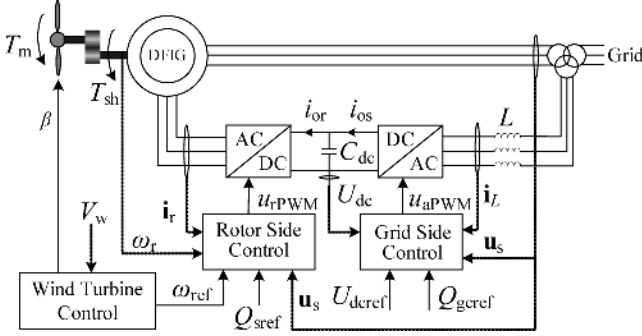
Fig. 1.   Schematic diagram of the DFIG WT system.

voltage protections. The key idea is to increase the generator rotor speed through proper control of the rotor side converter during a grid voltage dip. Different from conventional methods, the proposed control strategy is based on a simple concept to transform the unbalanced energy into the kinetic one, rather than being dissipated otherwise. For the grid side control scheme, a compensation item, which reflects the variation of the DC-link current of the rotor side converter, is added during the fault to smooth the fluctuations of the DC-link voltage. Compared with the LVRT solution in [19], the proposed control strategy for the grid side controller can effectively reduce the extremely high transient when the stator voltage dips to zero during faults. Simulation studies using Matlab/Simulink have been conducted on a 1.5-MW DFIG WT to validate the effectiveness of the proposed control strategy.

II. MODELING OF THE DFIG WIND TURBINE

The schematic diagram of a grid-connected DFIG WT system is shown in Fig. 1. The DFIG WT system, including the wind turbine, the drive train, the induction generator, the back-to-back PWM converters, and the control system, is connected to the grid through a transformer. The control system consists of two control levels including the WT control and the DFIG control. The WT level controls the output mechanical power of the wind turbine through the pitch angle and generates the reference value for the rotor speed of the DFIG based on the measured wind speed and optimum power-speed characteristic curve. A two-stage control strategy is used to implement the power optimization strategy below the rated wind speed, and the power limitation strategy above the rated wind speed [20]. The DFIG control level, including the rotor and grid side controllers, is to control the active and reactive power of the DFIG using the vector control technique. In Sections II-A–II-C, a detailed dynamic model of the DFIG WT will be presented.

A. Generator

The voltage equations of the stator and rotor circuits of the induction generator can be given in a d-q reference frame rotating at the synchronous speed [21], [22]

$$
\begin{cases}
u_{\mathrm{ds}} = R_{\mathrm{s}}i_{\mathrm{ds}} - \omega_{\mathrm{s}}\psi_{\mathrm{qs}} + \frac{1}{\omega_{\mathrm{b}}}\frac{d\psi_{\mathrm{ds}}}{dt} \\
u_{\mathrm{qs}} = R_{\mathrm{s}}i_{\mathrm{qs}} + \omega_{\mathrm{s}}\psi_{\mathrm{ds}} + \frac{1}{\omega_{\mathrm{b}}}\frac{d\psi_{\mathrm{qs}}}{dt} \\
u_{\mathrm{dr}} = R_{r}i_{\mathrm{dr}} - (\omega_{\mathrm{s}} - \omega_{r})\psi_{\mathrm{qr}} + \frac{1}{\omega_{\mathrm{b}}}\frac{d\psi_{\mathrm{dr}}}{dt} \\
u_{\mathrm{qr}} = R_{r}i_{\mathrm{qr}} + (\omega_{\mathrm{s}} - \omega_{r})\psi_{\mathrm{dr}} + \frac{1}{\omega_{\mathrm{b}}}\frac{d\psi_{\mathrm{qr}}}{dt}
\end{cases}
\tag{1}
$$

where $\mathbf{i}_{\mathrm{s}} = i_{\mathrm{ds}} + ji_{\mathrm{qs}}$ and $\mathbf{i}_{r} = i_{\mathrm{dr}} + ji_{\mathrm{qr}}$ are the stator and rotor current vectors, respectively; $\mathbf{u}_{\mathrm{s}} = u_{\mathrm{ds}} + ju_{\mathrm{qs}}$ and $\mathbf{u}_{r} = u_{\mathrm{dr}} + ju_{\mathrm{qr}}$ are the stator and rotor voltage vectors, respectively; $\mathbf{\Psi}_{\mathrm{s}} = \Psi_{\mathrm{ds}} + \Psi_{\mathrm{qs}}$ and $\mathbf{\Psi}_{r} = \Psi_{\mathrm{dr}} + j\Psi_{\mathrm{qr}}$ are the stator and rotor flux vectors, respectively; ω_{b}, ω_{s}, and ω_{r} are the base, stator, and rotor angular frequencies, respectively. The system model is written in the p.u. system with the time, t, in seconds.

B. Drive Train

When studying the dynamic stability of the DFIG WT, the two-mass model of the drive train is important due to the wind turbine shaft is relatively softer than the typical steam turbine shaft in conventional power plants [2]. The equations which represent the two-mass model of the drive train are expressed as

$$
\frac{d\omega_{r}}{dt} = \frac{1}{2H_{g}}(T_{sh} - T_{e} - B\omega_{r})
\tag{2}
$$

$$
\frac{d\theta_{\mathrm{t}}}{dt} = \omega_{\mathrm{b}}(\omega_{\mathrm{t}} - \omega_{r})
\tag{3}
$$

$$
\frac{d\omega_{\mathrm{t}}}{dt} = \frac{1}{2H_{\mathrm{t}}}(T_{\mathrm{m}} - T_{sh})
\tag{4}
$$

where ω_{t} is the wind turbine speed. H_{g} and H_{t} [SI unit (s)] are the generator and turbine inertia constants, respectively. B is the friction coefficient of the generator. θ_{t} is the shaft twist angle, which is in radian (rad.). The electromagnetic torque T_{e}, the shaft torque T_{sh}, and the mechanical torque T_{m}, which is the torque input of the wind turbine, are

$$
T_{e} = L_{\mathrm{m}}(i_{\mathrm{qs}}i_{\mathrm{dr}} - i_{\mathrm{ds}}i_{\mathrm{qr}})
\tag{5}
$$

$$
T_{sh} = K_{sh}\theta_{\mathrm{t}} + D_{sh}\omega_{\mathrm{b}}(\omega_{\mathrm{t}} - \omega_{r})
\tag{6}
$$

$$
T_{\mathrm{m}} = \frac{0.5\rho\pi R^{2}C_{\mathrm{p}}(\lambda,\beta)V_{\mathrm{w}}^{3}}{\omega_{\mathrm{t}}}
\tag{7}
$$

where ρ is the air density, R is the turbine radius, β is the pitch angle, V_{w} is the wind speed, C_{p} is the power coefficient, and

$$
C_{\mathrm{p}} = 0.22\left(\frac{116}{\lambda_{\mathrm{i}}} - 0.4\beta - 5\right)e^{-12.5/\lambda_{\mathrm{i}}}
\tag{8}
$$

$$
\lambda_{\mathrm{i}} = \frac{1}{\frac{1}{(\lambda+0.08\beta)} - \frac{0.035}{(\beta^{3}+1)}}
\tag{9}
$$

where $\lambda = \omega_{\mathrm{t}}R/V_{\mathrm{w}}$ is the blade tip speed ratio, $C_{\mathrm{p}}(\lambda,\beta)$ has a maximum value $C_{\mathrm{p}}^{\mathrm{max}}$ for the optimal tip speed ratio λ_{opt} and optimized pitch angle β_{opt}. The wind turbine control is achieved by driving the generator/turbine speed along the optimum power-speed characteristic curve, illustrated in Fig. 2 [20], which corresponds to the maximum energy capture from the wind. In this curve, when the wind speed is larger than the cut-in wind speed $V_{\mathrm{w}}^{\mathrm{cut-in}}$ and less than the lower limit $V_{\mathrm{w}}^{\mathrm{min}}$ (zone A–B), the generator rotor speed reference for the rotor side controller ω_{ref} is set as the minimal value $\omega_{r}^{\mathrm{min}}$, $\omega_{r}^{\mathrm{min}} = 0.7$ p.u., to ensure the generator slip smaller than 0.3. When the wind speed is between the lower limit and the rated value $V_{\mathrm{w}}^{\mathrm{rated}}$ (zone B–C), the DFIG is operated in the variable speed mode, where β is kept constant to β_{opt} (usually $\beta_{\mathrm{opt}} = 0$), while
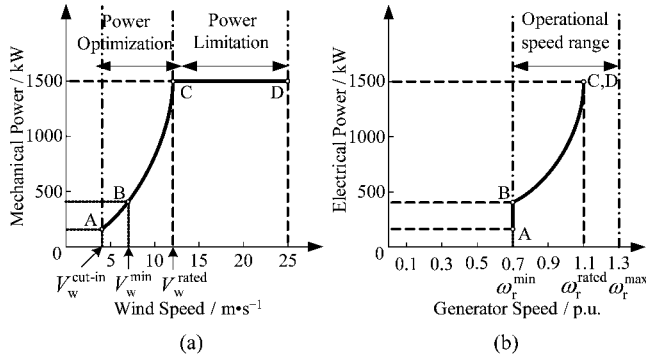
Fig. 2. Two static curves used in the design of the DFIG WT. (a) Mechanical power versus wind speed. (b) Electrical power versus generator speed.
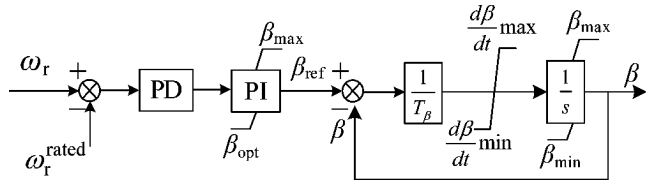

Fig. 3. Schematic diagram of the pitch control.

λ is tuned to λ_{opt} over different wind speeds by adapting the generator speed to ω_{ref}, which can be obtained by substituting $\lambda = \omega_t R / V_w$ into (7), expressed by [23]

$$\omega_{\text{ref}} = \sqrt{\frac{T_m}{K_{\text{opt}}}} \qquad (10)$$

where $K_{\text{opt}} = \rho \pi R^5 C_p^{\text{max}} / 2\lambda_{\text{opt}}^3$ is the optimal constant of wind turbine. Therefore, C_p can be maintained at C_p^{max} and the maximal power is achieved by tracking ω_{ref} in (10). When the wind speed is higher than the rated value (zone C-D), ω_{ref} is set as the rated value of the generator speed ω_r^{rated}, the over rated turbine power production will be restrained by the pitch control, which can therefore limit the over-speed of the generator.

C. Pitch Control

The pitch angle of the blade is controlled to optimize the power extraction of the WT as well as to prevent over rated power production in high wind. The pitch servo is modeled as

$$\frac{d\beta}{dt} = \frac{1}{T_\beta}(\beta_{\text{ref}} - \beta). \qquad (11)$$

The pitch control scheme is shown in Fig. 3 [2]. When the generator speed exceeds ω_r^{rated}, the pitch control is active and the pitch angle is tuned so that the turbine power can be restricted to its rated value.

III. PROPOSED LOW-VOLTAGE RIDE-THROUGH STRATEGY

A. Overview of the Proposed Control Strategy

When the power grid is subject to, e.g., a short-circuit fault, the bus voltage at the PCC drops, and therefore introducing undesirable transients in the stator and rotor currents. The low voltage also prevents the full transmission of generated active power from the WT, leading to significantly increased fluctuations of the currents and voltages in the DFIG system. In order to protect the power electronics devices that are sensitive to over-currents and over-voltages, the purpose of introducing the LVRT strategy is to ensure the DFIG can stay connected to the faulted grid by effectively limiting the stator and rotor circuit currents as well as the DC-link voltage.

The conventional crowbar control realizes the LVRT protection by blocking the rotor side converter circuit and introducing additional rotor winding resistances that actually dissipate the produced energy. In contrast, the proposed control strategy can transform the additional output power into the WT kinetic energy by temporarily increasing the generator rotor speed during the grid faults, thus effectively limiting the oscillations in the currents. If the rotor speed increases above the rated value, the pitch control will be triggered to decrease the power extraction from the wind. This can restrict the over-speed of the rotor and therefore limit the excessive mechanical stress applied to the turbine system. Moreover, a compensation item, which reflects the variation of the DC-link current of the rotor side converter, is added to the grid side control scheme during the fault so as to smooth the fluctuation of the DC-link voltage.

The proposed control strategy makes full use of existing resources within the DFIG WT system to realize the LVRT without the need of additional components like the crowbar. It can effectively protect the power electronics devices against current and voltage fluctuations during grid faults to ensure the LVRT of the DFIG. Several advantages can be achieved by using the new control strategy. From the energy perspective, the new control strategy can absorb the additional output power during the faults that will be otherwise dissipated in the crowbar based control. Notably, the increased kinetic energy of the WT can be released into the grid slowly after the fault clearance. From the control perspective, the new control strategy can erasure the back-to-back converters well connected to the DFIG as well as the grid without loss of the controllability during the faults. This potentially can enable both active and reactive supports to the faulted grids from WT which is difficult for the crowbar based control. The detailed control scheme will be illustrated in Sections III-B and III-C, and the simulation validation will be given in Section IV.

B. Control of Rotor Side Converter (RSC)

In normal operation, the control scheme of the RSC is illustrated in Fig. 4. In order to decouple the electromagnetic torque and the rotor excitation current, the induction generator is controlled in the stator-flux oriented reference frame, which is a synchronously rotating reference frame, with its d-axis oriented along the stator-flux vector position (in this paper, the stator-flux vector is calculated using $\mathbf{u}_s$) [23]. The typical proportional-integral (PI) controllers are used for regulation in the rotor speed and reactive power (outer) control loops as well as the rotor current (inner) control loops. The values of ω_{ref}, generated by the wind turbine control level, at different operation conditions have been defined in Section II.

When a short-term low-voltage fault occurs, the incoming power from the wind and the power flowing into the grid are

Fig. 4.   Control scheme of the rotor side converter in normal operation.

Fig. 6.   Control scheme of the grid side converter in normal operation.

Fig. 5.   Control scheme of the rotor side converter during a grid fault.

imbalanced instantaneously, resulting in the transient excessive currents in the rotor and stator circuits. Therefore from the energy balance point of view, the key point of suppressing the over-currents in the rotor and stator circuits is to reduce the imbalanced energy flowing through the DFIG WT system.

When at least one of the monitored parameters, including the rotor current, stator current, DC-link voltage, and grid voltage, exceeds its respective protection setting due to the grid fault, the proposed LVRT control strategy will be triggered. With this control strategy, the rotor side controller will increase the generator rotor speed by reducing the generator torque to zero during the fault, in order to absorb and convert the incoming energy from the wind into the kinetic energy in the WT inertia. The increased kinetic energy can be transformed and released into the grid after the fault clearance. The control scheme of the RSC against grid faults is illustrated in Fig. 5.

The parameters of the PI controllers are tuned using the pole placement methodology [24] in order to ensure the rising times of the inner and outer control loops are less than 10 ms and 50 ms, respectively; and the maximum deviations of the inner and outer control loops are both less than 20%.

The new control strategy will not cause excessive mechanical stress to the WT system. When the DFIG WT is operating at or close to the rated speed, the acceleration due to the proposed control scheme during the fault may accelerate the wind turbine speed above its rated value. This can increase the thrust and centrifugal forces, applied to the rotor construction that may endanger the wind turbine mechanical system [2]. However, the over-speed of the WT can be effectively restrained by the pitch control, which will be activated immediately when the rotor speed becomes higher than the rated value. Moreover, the duration of the over-speed is short, due to the short duration and rare occurrence of grid faults. According to the expressions of the thrust and centrifugal forces in [2], the negative impacts due

to the proposed control strategy can be little to the safe operation of WTs. This analysis will be verified by the simulation results in Section IV.

C. Control of Grid Side Converter (GSC)

Fig. 6 shows the control scheme of the GSC in normal operation, where $\mathbf{u}_a$ and $\mathbf{i}_L$ are the grid-side converter voltage vector and the grid-side inductor current vector, respectively. In order to obtain the independent control of active and reactive power flowing between the grid and the GSC, the converter control operates in the grid-voltage oriented reference frame, which is a synchronously rotating reference frame, with its d-axis oriented along the grid-voltage vector position [23]. Similarly, the typical PI controllers are used for regulation in the DC-link voltage (outer) control loop and the grid side inductor current (inner) control loops.

The equation which describes the dynamic behavior of the DC-link capacitor can be expressed as

$$C_{dc}\frac{dU_{dc}}{dt} = i_{os} - i_{or} \qquad (12)$$

where i_{os} and i_{or} are the DC-link currents of the grid and rotor side converters, respectively. Neglecting the losses in the inductor resistances and power electronics converters, we have

$$i_{os} = \frac{\sqrt{3}m}{\sqrt{2}}i_{dL}$$
$$i_{or} = \frac{P_r}{U_{dc}} \qquad (13)$$

where P_r is the magnitude of the active power of the generator rotor.

In normal operation, when the power flowing through the grid and rotor side converters is balanced, i_{os} is equal to i_{or}, so the DC-link voltage is constant. When the grid voltage dips, i_{os} may not be equal to i_{or}, due to the instantaneous unbalanced power flow between the grid and rotor side converters, and therefore the DC-link voltage may fluctuate. In [19] in order to reduce the fluctuation of the DC-link voltage, the item (P_r/u_{ds}) reflecting the instantaneous variation of the output power of the rotor side controller is directly set as the reference of the i_{dL} during the grid fault. However, the stator voltage u_{ds} may reduce to zero during the grid fault. This will introduce an extremely high transient value of i_{dL}.

In this paper, when the rotor current, stator current, DC-link voltage, or grid voltage exceeds its respective relay setting due
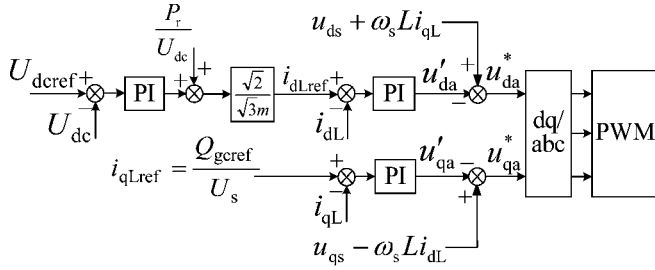
Fig. 7. Control scheme of the grid side converter during a grid fault.
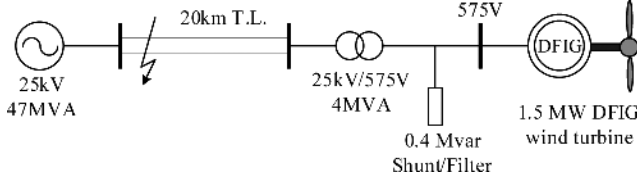

Fig. 8. Single line diagram for the studied system.

to the grid voltage dip, the term (P_r/U_{dc}) describing i_{or} is represented as a disturbance to compensate the instantaneous rotor power in the control scheme. In such a way, the i_{dL} can be regulated smoothly during a grid fault. The detailed control scheme of the GSC during the grid fault is shown in Fig. 7.

Similarly, the pole placement methodology is applied to design the PI controller parameters of the grid side controller so as to obtain the same rising time and maximum deviation as the rotor side controller.

IV. ANALYSIS OF LOW-VOLTAGE RIDE-THROUGH STRATEGIES

The DFIG WT under study is connected to the grid transmission level via a radial link as shown in Fig. 8. In order to evaluate the proposed control strategy, the complete DFIG WT system model has been developed and simulated in Matlab/Simulink environment. The components of the simulation model are built with standard electrical component blocks from the SimPowerSystems block in Matlab/Simulink library. The parameters of the studied DFIG WT, which are mostly based on existing information from industries and literatures, are listed in the Appendix.

Three different control strategies of LVRT on the performance of the studied DFIG WT during different symmetrical three-phase short-circuit faults are investigated to study their effects, including

Strategy A: The conventional protective system equipped with crowbar and DC-link chopper.
Strategy B: The proposed control strategy of RSC only.
Strategy C: The proposed control strategy of RSC and GSC.

The DFIG WT with the crowbar and DC chopper protection circuits of the strategy A is shown in Fig. 9. The crowbar circuit includes the controllable switches and resistors. The crowbar resistors are all chosen as $40R_r$. The DC chopper resistor is selected as 0.5 p.u. The protection thresholds of rotor and stator currents are both set to 1.5 p.u. The detailed scheme of the crowbar protection is described in [2].
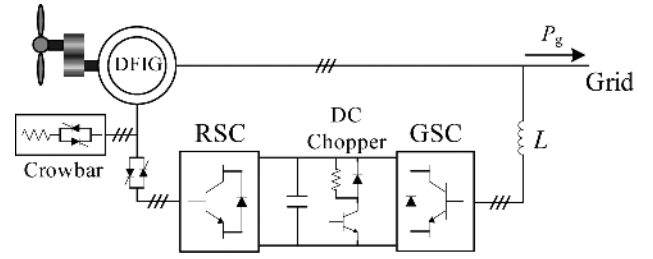

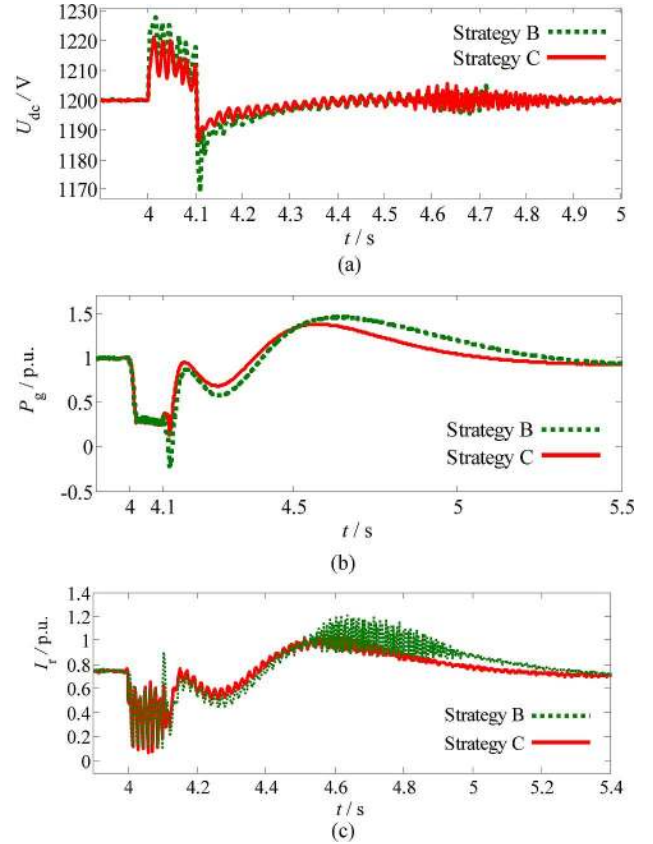Fig. 9. DFIG WT with the crowbar and DC chopper protection circuits.

Fig. 10. Simulated transient responses of the studied DFIG WT at wind speed of 13 m/s with the control strategy B and C during a 100-ms fault. (a) DC-link voltage. (b) Active power to the grid. (c) Magnitude of the rotor current.

A. Comparing the LVRT Behaviors With Strategy B and C

At time $t = 4$ s, a three-phase short-circuit fault with a duration of 100 ms occurs in the transmission power grid and the PCC voltage drops to about 0.2 p.u. The simulated transient behaviors of the studied DFIG WT operating at the wind speed of 13 m/s and installed with the control strategy B and C are shown in Fig. 10.

Fig. 10 shows that with the strategy B, the fluctuation of the DC-link voltage is not damped sufficiently. As the rotor current control might be affected by the DC-link voltage fluctuation, the transient performances of active power and rotor current controlled by the strategy B are worse than with the strategy C. Due to the additional grid side control scheme in the strategy C, the fluctuation of DC-link voltage has been effectively reduced and the LVRT behavior of the DFIG WT is better than with the strategy B. This is because when the wind speed is

13 m/s, which is higher than the rated wind speed, the DFIG WT will be operating at the rated rotor speed accordingly. The over-speed of the WT caused by the proposed control strategy of the RSC can be effectively restrained by the pitch control. This will limit the transformation of the electric energy into the kinetic one. So when the pitch control is triggered, introducing the compensation term P_r/U_{dc} in the grid side controller can help reducing the over-voltage on the DC bus. Hence the necessity of including the GSC in the proposed control strategy has been justified in order to achieve a better LVRT performance of the DC-link voltage during the grid faults.

B. LVRT Behaviors at Low Wind Speed

In the following analyses, in order to meet the ride-through requirement of a widely referred grid code [25], two typical three-phase short-circuit faults are imposed on the transmission power grid at $t = 4$ s, the PCC voltage drop to 0 for 150 ms and to 15% of its nominal value for 625 ms, respectively. The LVRT capability of the proposed control strategy C is simulated and compared with the performance of the conventional crowbar protection based the strategy A.

The LVRT behaviors of the studied DFIG WT operating at wind speed of 8 m/s, when the voltage at the PCC drops to 0 for 150 ms are shown in Fig. 11. During the fault, the acceleration of the generator rotor speed with the control strategy C is faster than the cases with the strategy A. The active acceleration of the rotor speed in the strategy C can transform the additional energy into the kinetic one; therefore, the fluctuations of the active power, reactive power, stator and rotor current, and DC-link voltage are significantly reduced than the case of the crowbar based strategy A. For example, the rotor current in the case with the strategy A shoots up to 2.2 p.u. at the instant of the grid fault, while the proposed control strategy C can suppress the rotor current no more than 0.96 p.u., which is below the activation threshold of the crowbar. Therefore, the proposed control strategy can enable the WT to ride through this fault even without triggering the crowbar protection. It is also observed that after the fault clearance, the rotor speed decreases back to the reference value and the oscillations are well damped under the proposed control strategy C.

Fig. 12 shows the LVRT behaviors of the studied DFIG WT operating at wind speed of 8 m/s, when the voltage at the PCC drops to 15% for 625 ms. This illustrates that with the proposed control strategy C, the DFIG WT can remain connected to the grid during a longer duration of fault without triggering the crowbar protection and the LVRT behaviors of the active power, reactive power, stator and rotor current, and DC-link voltage are better than the case with the strategy A.

C. LVRT Behaviors at High Wind Speed

Fig. 13 presents the LVRT behaviors of the studied DFIG WT operating at wind speed of 13 m/s with the conventional crowbar control based strategy A and with the new control strategy C, when the voltage at the PCC drops to 0 for 150 ms.

When the DFIG WT is operating at the wind speed of 13 m/s, which is higher than the rated wind speed, the DFIG WT is operating at the rated rotor speed. The acceleration of the rotor
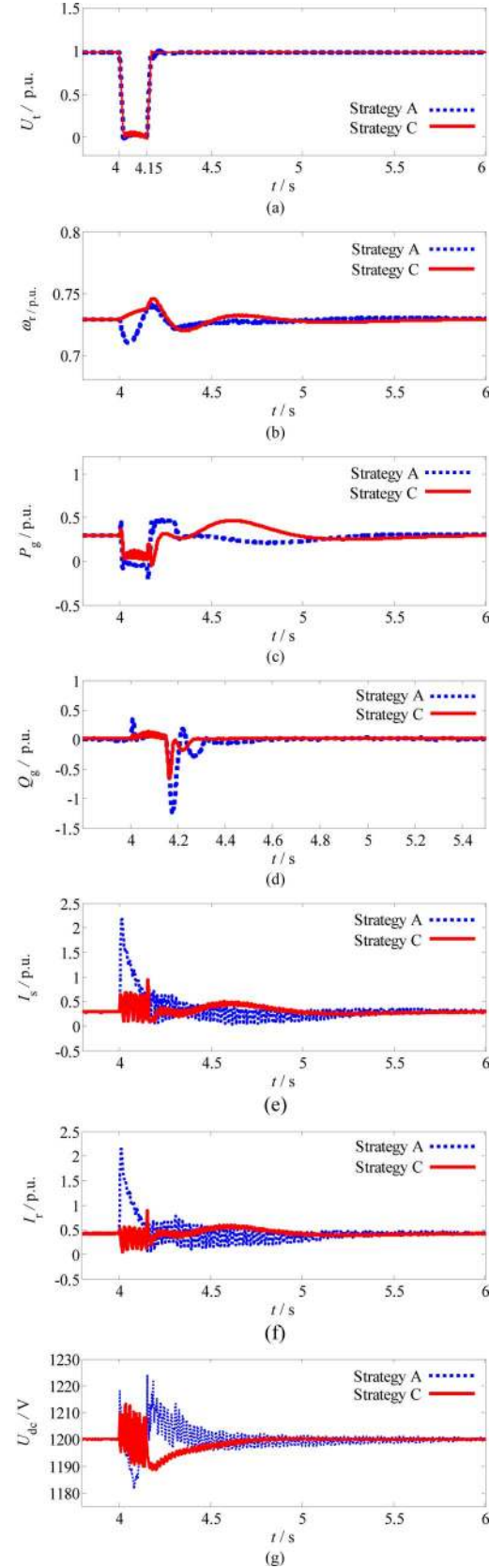

Fig. 11. Simulated transient responses of the studied DFIG WT at wind speed of 8 m/s with the control strategies A (crowbar) and C (the newly proposed LVRT strategy), when the voltage at the PCC drops to 0 for 150 ms. (a) Voltage at the DFIG terminal. (b) Generator rotor speed. (c) Active power to the grid. (d) Reactive power to the grid. (e) Magnitude of the stator current. (f) Magnitude of the rotor current. (g) DC-link voltage.
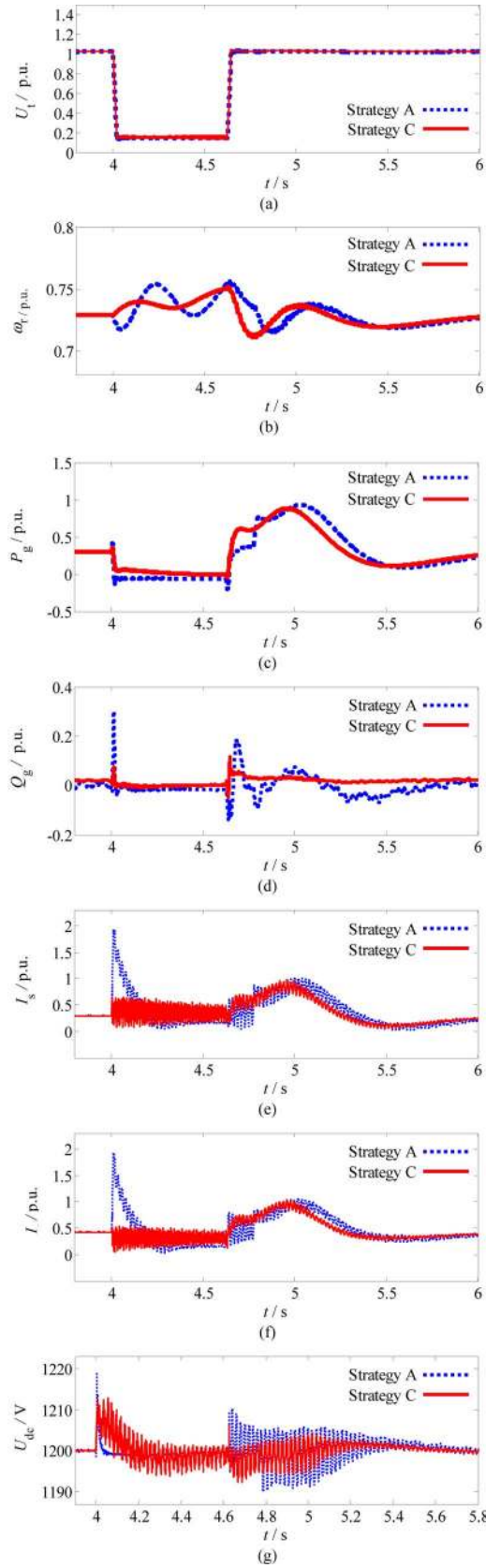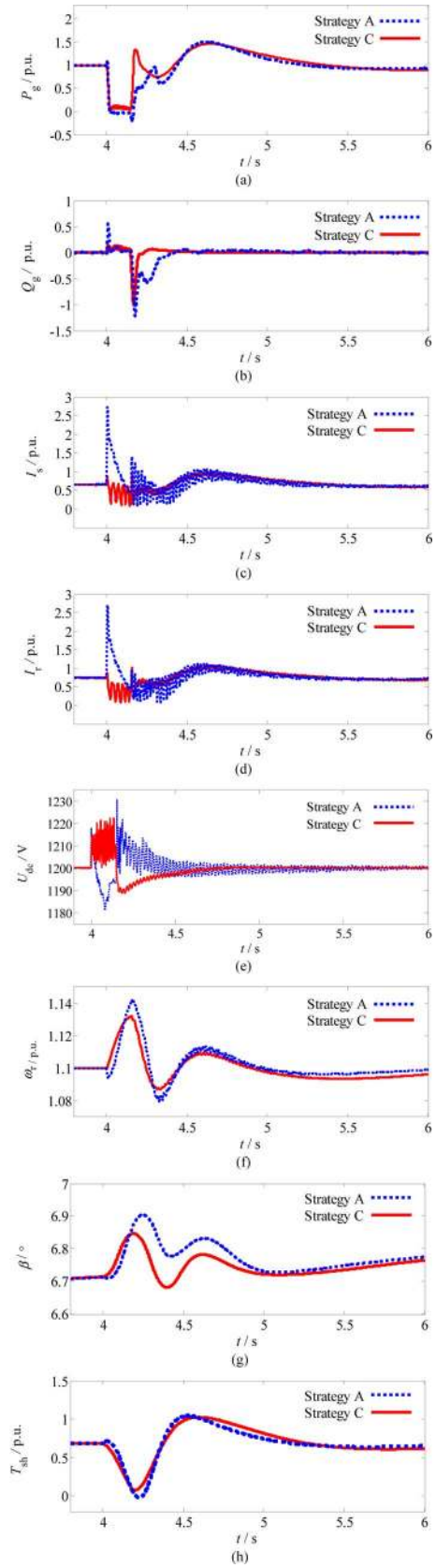
Fig. 12. Simulated transient responses of the studied DFIG WT at wind speed of 8 m/s with the control strategies A (crowbar) and C (the newly proposed LVRT strategy), when the voltage at the PCC drops to 15% of its nominal value for 625 ms. (a) Voltage at the DFIG terminal. (b) Generator rotor speed. (c) Active power to the grid. (d) Reactive power to the grid. (e) Magnitude of the stator current. (f) Magnitude of the rotor current. (g) DC-link voltage.

Fig. 13. Simulated transient responses of the studied DFIG WT at wind speed of 13 m/s with the control strategies A (crowbar) and C (the newly proposed LVRT strategy), when the voltage at the PCC drops to 0 for 150 ms. (a) Active power to the grid. (b) Reactive power to the grid. (c) Magnitude of the stator current. (d) Magnitude of the rotor current. (e) DC-link voltage. (f) Generator rotor speed. (g) Pitch angle. (h) Shaft torque.

speed due to the proposed control scheme during the fault will make the rotor speed above its rated value, which will trigger the pitch control immediately. This can limit the transformation of the electric energy into the kinetic one. Therefore in Fig. 13(e), (f), and (h), the differences of the DC-link voltage, the rotor speed, and shaft torque during the fault between the strategies A and C are smaller than the case when the DFIG WT operating at low wind speed. However, the transient behaviors of the active and reactive power, stator and rotor current, and pitch angle in the case of the proposed control strategy C are still observed better than with the conventional crowbar protection. Especially, the proposed control strategy can suppress the transient stator and rotor currents lower than the crowbar threshold; thus, the DFIG can maintain uninterrupted control of active and reactive power, potentially enabling the grid supporting services during the fault.

Fig. 14 shows the LVRT behaviors of the studied DFIG WT operating at wind speed of 13 m/s, when the voltage at the PCC drops to 15% for 625 ms. This illustrates that with the proposed control strategy C, the DFIG WT operating at high wind speed can remain connected to the grid during a longer duration of fault without triggering the crowbar protection and has better LVRT behaviors of the active power, reactive power, stator and rotor current, DC-link voltage, pitch control, and shaft torque than the case with conventional crowbar protection.

In Figs. 13(f) and 14(f), the rotor speed slightly exceeds the rated value. However, the maximum over-speed is only 2.72% and the period of the whole violation is 230 ms when the voltage at the PCC drops to 0 for 150 ms; the maximum over-speed is only 6.06% and the period of the whole violation is 1.5 s when the voltage at the PCC drops to 15% of its nominal value for 625 ms. The corresponding increase of the thrust and centrifugal forces due to the over-speed is little according to their expressions [2], and the over-speed duration is short, indicating a very little impact on the wind turbine construction, which verifies the analysis in Section III.

V. CONCLUSIONS

High penetration of WTs imposes a significant challenge to the safe operation of power systems. To ensure the security of electricity supply with substantial wind power, the WTs must ride through and even contribute to supporting the grid operation under the fault conditions.

This paper proposes a new and efficient control strategy for both the rotor and grid side converters to improve the LVRT capability of the DFIG WT. The new control strategy enables the DFIG to continue the electricity production, and absorb the excessive energy by increasing the generator rotor speed temporarily when a fault occurs at, e.g., the PCC. The new strategy also introduces a compensation item to the grid side controller in order to suppress the DC-link over-voltage during the faults.

The simulation results show that the proposed control strategy is able to effectively suppress the transients in the rotor circuit current and the DC-link voltage. Compared with the conventional crowbar protection, the DFIG WT installed with the proposed control strategy gives a better transient behavior in event of short-term grid voltage dip. By using the new control strategy,
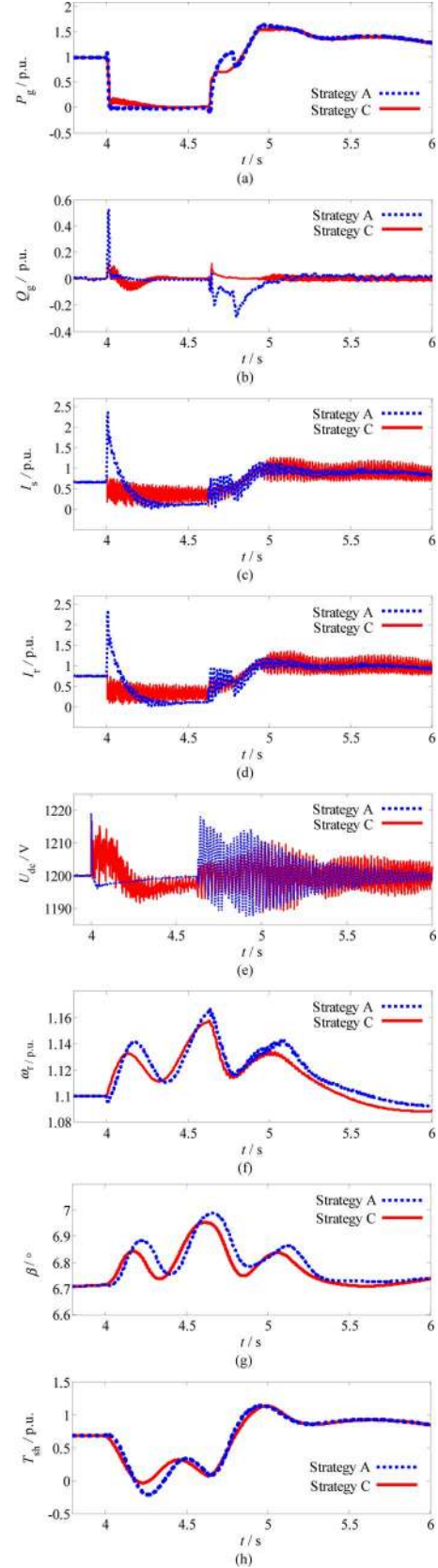

Fig. 14. Simulated transient responses of the studied DFIG WT at wind speed of 13 m/s with the control strategies A (crowbar) and C (the newly proposed LVRT strategy), when the voltage at the PCC drops to 15% of its nominal value for 625 ms. (a) Active power to the grid. (b) Reactive power to the grid. (c) Magnitude of the stator current. (d) Magnitude of the rotor current. (e) DC-link voltage. (f) Generator rotor speed. (g) Pitch angle. (h) Shaft torque.

little impact will be resulted to the WT mechanical construction and the occurrence of the crowbar interruption can also be minimized.

APPENDIX

The parameters of the studied DFIG WT are as follows:

Wind turbine: cut-in wind speed: 4 m/s; lower limit of the wind speed: $V_w^{\min} = 7$ m/s; rated wind speed: 12 m/s; inertia constant: $H_t = 3$ s; damping coefficient: $D_{sh} = 0.01$ p.u.; shaft stiffness coefficient: $K_{sh} = 0.5$ p.u.; time constant of the pitch servo: $T_\beta = 0.25$ s.

DFIG: rated power: 1.5 MW; rated voltage: 575 V; rated current; 1505 A; rated rotor speed: $\omega_r^{\text{rated}} = 1.1$ p.u. (with the synchronous speed as the base value); inertia constant: $H_g = 0.5$ s; friction coefficient: $B = 0.01$ p.u.; stator resistance: $R_s = 0.00706$ p.u.; rotor resistance: $R_r = 0.005$ p.u.; stator leakage inductance: $L_{ls} = 0.171$ p.u.; rotor leakage inductance: $L_{lr} = 0.156$ p.u.; mutual inductance: $L_m = 3.5$ p.u.

Converters: resistance of grid side inductor: $R_L = 0.003$ p.u.; inductance of grid side inductor: $L = 0.3$ p.u.; DC-link capacitor: $C_{dc} = 0.06F$.

REFERENCES

[1] A. Thomas, *Wind Power in Power Systems*. New York: Wiley, 2005.

[2] V. Akhmatov, *Induction Generators for Wind Power*. Brentwood, CA: Multi-Science, 2005.

[3] I. Erlich, J. Kretschmann, J. Fortmann, S. Mueller-Engelhardt, and H. Wrede, "Modeling of wind turbines based on doubly-fed induction generators for power system stability studies," *IEEE Trans. Power Syst.*, vol. 22, no. 3, pp. 909–919, Aug. 2007.

[4] J. Yang, J. E. Fletcher, and J. O'Reilly, "A series dynamic resistor based converter protection scheme for doubly-fed induction generator during various fault conditions," *IEEE Trans. Energy Convers.*, vol. 25, no. 2, pp. 422–432, Jun. 2010.

[5] A. H. Kasem, E. F. EI-Saadany, H. H. EI-Tamaly, and M. A. A. Wahab, "An improved fault ride-through strategy for doubly fed induction generator-based wind turbines," *IET Renew. Power Gen.*, vol. 2, no. 4, pp. 201–214, Dec. 2008.

[6] S. Foster, L. Xu, and B. Fox, "Coordinated reactive power control for facilitating fault ride through of doubly fed induction generator- and fixed speed induction generator-based wind farms," *IET Renew. Power Gen.*, vol. 4, no. 2, pp. 128–138, Mar. 2008.

[7] L. Peng, B. Francois, and Y. Li, "Improved crowbar control strategy of DFIG based wind turbines for grid fault ride-through," in *Proc. IEEE 24th Annu. Applied Power Electronics Conf. Expo.*, Washington, DC, Feb. 2009, pp. 1932–1938.

[8] M. B. C. Salles, J. R. Cardoso, A. P. Grilo, C. Rahmann, and K. Hameyer, "Control strategies of doubly fed induction generators to support grid voltage," in *Proc. IEEE Int. Electric Machines and Drives Conf.*, May 2009, pp. 1551–1556.

[9] J. López, E. Gubía, E. Olea, J. Ruiz, and L. Marroyo, "Ride through of wind turbines with doubly fed induction generator under symmetrical voltage dips," *IEEE Trans. Ind. Electron.*, vol. 56, no. 10, pp. 4246–4254, Oct. 2009.

[10] L. G. Meegahapola, T. Littler, and D. Flynn, "Decoupled-DFIG fault ride-through strategy for enhanced stability performance during grid faults," *IEEE Trans. Sustain. Energy*, vol. 1, no. 3, pp. 152–162, Oct. 2010.

[11] D. Xiang, L. Ran, P. J. Tavner, and S. Yang, "Control of a doubly-fed induction generator in a wind turbine during grid fault ride-through," *IEEE Trans. Energy Convers.*, vol. 21, no. 3, pp. 652–662, Sep. 2006.

[12] M. Rathi and N. Mohan, "A novel robust low voltage and fault ride through for wind turbine application operating in weak grids," in *Proc. IEEE Industrial Electronics Society Conf.*, Nov. 2005, pp. 6–10.

[13] A. Hansen and G. Michalke, "Fault ride-through capability of DFIG wind turbines," *Renew. Energy*, vol. 32, no. 9, pp. 1594–1610, Jul. 2007.

[14] J. Lopez, P. Sanchis, X. Roboam, and L. Marroyo, "Dynamic behavior of the doubly fed induction generator during three-phase voltage dips," *IEEE Trans. Energy Convers.*, vol. 22, no. 3, pp. 709–717, Sep. 2007.

[15] L. Xu and P. Cartwright, "Direct active and reactive power control of DFIG for wind energy generation," *IEEE Trans. Energy Convers.*, vol. 21, no. 3, pp. 750–758, Sep. 2007.

[16] M. Rahimi and M. Parniani, "Transient performance improvement of wind turbines with doubly fed induction generators using nonlinear control strategy," *IEEE Trans. Energy Convers.*, vol. 25, no. 2, pp. 514–525, Jun. 2010.

[17] F. K. A. Lima, A. Luna, P. Rodriguez, E. H. Watanabe, and F. Blaabjerg, "Rotor voltage dynamics in the doubly fed induction generator during grid faults," *IEEE Trans. Power Electron.*, vol. 25, no. 1, pp. 118–130, Jan. 2010.

[18] J. Liang, W. Qiao, and R. G. Harley, "Feed-forward transient current control for low-voltage ride-through enhancement of DFIG wind turbines," *IEEE Trans. Energy Convers.*, vol. 25, no. 3, pp. 836–843, Sep. 2010.

[19] J. Yao, H. Li, Y. Liao, and Z. Chen, "An improved control strategy of limiting the DC-link voltage fluctuation for a doubly fed induction wind generator," *IEEE Trans. Power Electron.*, vol. 23, no. 3, pp. 1205–1213, May 2008.

[20] A. D. Hansen, P. Sørensen, F. Iov, and F. Blaabjerg, "Control of variable speed wind turbines with doubly-fed induction generators," *Wind Eng.*, vol. 28, no. 4, pp. 411–434, 2004.

[21] F. Mei and B. C. Pal, "Modal analysis of grid-connected doubly fed induction generators," *IEEE Trans. Energy Convers.*, vol. 22, no. 3, pp. 728–736, Sep. 2007.

[22] F. Wu, X. P. Zhang, K. Godfrey, and P. Ju, "Small signal stability analysis and optimal control of a wind turbine with doubly fed induction generator," *IET Gen., Transm., Distrib.*, vol. 1, no. 5, pp. 751–760, Sep. 2007.

[23] R. Pena, J. C. Clare, and G. M. Asher, "Doubly fed induction generator using back-to-back PWM converters and its application to variable speed wind-energy generation," *Proc. Inst. Elect. Eng., Elect. Power Appl.*, vol. 143, no. 3, pp. 231–241, May 1996.

[24] J. H. Chow, "A pole-placement design approach for systems with multiple operating conditions," *IEEE Trans. Autom. Control*, vol. 35, no. 2, pp. 278–288, Feb. 1990.

[25] M. Tsili and S. Papathanassiou, "A review of grid code technical requirements for wind farms," *IET Renew. Power Gen.*, vol. 3, no. 3, pp. 308–332, Sep. 2009.

Lihui Yang received the Ph.D. degree in electrical engineering from Xi'an Jiaotong University, Xi'an, China, in 2010.

During 2008–2009, she was a visiting Ph.D. student with the Centre for Electric Technology, Technical University of Denmark, Lyngby, Denmark. She was a Research Assistant with Hong Kong Polytechnic University during June–November 2010. She is currently an Assistant Professor with Xi'an Jiaotong University. Her research interests include stability and control of wind power generation.

Zhao Xu (S'00–M'06) received the Ph.D. degree in electrical engineering from The University of Queensland, Brisbane, Australia, in 2006.

From 2006–2009, he was an Assistant and later Associate Professor with the Centre for Electric Technology, Technical University of Denmark, Lyngby, Denmark. Since 2010, he has been with Hong Kong Polytechnic University. His research interests include demand side, grid integration of wind power, electricity market planning and management, and AI applications.

Jacob Østergaard (M'95,–SM'09) is Professor and Head of the Centre for Electric Technology, Department of Electrical Engineering, Technical University of Denmark, Lyngby, Denmark. His research interests include integration of renewable energy, control architecture for future power system, and demand side.

Prof. Østergaard is serving in several professional organizations including the EU SmartGrids advisory council.

Zhao Yang Dong (M'99–SM'06) received the Ph.D. degree from The University of Sydney, Sydney, Australia, in 1999.

He is Ausgrid Chair of Intelligent Electricity Networks at the University of Newcastle, Newcastle, Australia. He previously held academic positions with Hong Kong Polytechnic University, and The University of Queensland, Brisbane, Australia. He also held industrial positions with Transend Networks, Tasmania, Australia. His research interest includes power system planning, smart grid, power system security assessment, power system stability and control, power system load modeling, electricity market, and computational intelligence and its application in power engineering.

Dr. Dong is an editor of the IEEE TRANSACTIONS ON SMART GRID.

Kit Po Wong (M'87–SM'90–F'02) He received the M.Sc, Ph.D., and higher doctorate D.Eng degrees from the University of Manchester, Institute of Science and Technology, Manchester, U.K., in 1972, 1974, and 2001, respectively.

He was with The University of Western Australia, Perth, Australia, from 1974 until 2004 and presently an Adjunct Professor there. From 2002 to 2011, he was Chair Professor and Head (2002–2007) of the Department of Electrical Engineering, The Hong Kong Polytechnic University. His current research interests include power system analysis, planning and operation, as well as computation intelligence applications to power engineering.

Prof. Wong received three Sir John Madsen Medals (1981, 1982, and 1988) from the Institution of Engineers Australia, the 1999 Outstanding Engineer Award from IEEE Power Chapter Western Australia, and the 2000 IEEE Third Millennium Award. He was General Chairman of IEEE/CSEE PowerCon2000, and of IEE (IET) APSCOM 2003 and 2009. He was one of the Founders of the international DRPT conference series. Presently, he is serving as Editor-in-Chief of the IEEE PES LETTERS. He was an Editor-in-Chief of *IEE Proceedings in Generation, Transmission and Distribution* and Editor (Electrical) of the *Transactions of Hong Kong Institution of Engineers*. He is a Fellow of IET, HKIE, and IEAust.